Journal of CO2 Utilization 69 (2023) 102421

Contents lists available at ScienceDirect

Journal of CO2 Utilization

journal homepage: www.elsevier.com/locate/jcou

Integrated techno-economic and life cycle assessment of a novel algae-based coating for direct air carbon capture and sequestration

Garrett M. Cole [a], Jonah M. Greene [a,1], Jason C. Quinn [a], Beth McDaniel [b], Lisa Kemp [b], David Simmons [b], Tyler Hodges [b,c], David Nobles [d], Taylor L. Weiss [e], John McGowen [e], Steve McDaniel [b,*]

[a] Sustainability Science LLC, 30940 Hummingbird Lane, Steamboat Springs, CO 80487, United States
[b] Reactive Surfaces Ltd, 300 West Avenue, Austin, TX 78701, United States
[c] The University of Alabama, 1325 Hackberry Ln, Tuscaloosa, AL 35401, United States
[d] University of Texas at Austin, 205 W 24th ST, Austin, TX 78712, United States
[e] Arizona Center for Algae Technology and Innovation, 7418 Innovation Way S #103, Mesa, AZ 85212, United States

ARTICLE INFO

Keywords:
Carbon capture and storage
Techno-economic analysis
Life cycle assessment
Carbon capture coating
Carbon fixation

ABSTRACT

Direct air carbon capture and storage (DACCS) systems are expected to play an important role in fighting global warming. While existing DACCS technologies have demonstrated CO_2 removal rates at or below the kiloton scale, high capital costs and significant energy demands represent hurdles in achieving large scale deployment. This study evaluates a novel biomimetic coating primarily consisting of a hydrogel seeded with microalgae biomass printed on a polyethylene substrate. The coating has been developed to exploit the high photosynthetic rates of microalgae to fix atmospheric CO_2 into cellulose using incident solar energy. The carbon embodied in the cellulose material is converted to biochar through pyrolysis to ensure durable carbon sequestration without the need for underground storage. The proposed system offers many advantages including modularity and scalability, the potential for high water retention rates, and long periods of operation with minimal maintenance and management. Three scenarios were evaluated using conservative, baseline, and optimistic assumptions to capture the true range in performance of the system. Results from the modeling work show a carbon removal efficiency ranging from 51% to 73% and carbon capture and sequestration costs of $702–$1585 per tonne CO_2 sequestered. Furthermore, the modular design of the coated substrate system and utilization of solar energy supports the rapid upscaling necessary to meet mid-century carbon removal goals. Discussion focuses on the key performance drivers of the system and the challenges and feasibility of meeting target metrics to support economic and environmental sustainability.

1. Introduction

Anthropogenic greenhouse gas (GHG) emissions have caused the global temperature to rise approximately 1.18 °C since the 19th century resulting in a multitude of devastating environmental impacts. Some of these impacts include warming oceans and shrinking ice sheets, sea level rise, loss of biodiversity, and increased severity and frequency of natural disasters and wild fires [1]. Outlined in the 6th Assessment Report from the International Panel on Climate Change, the best path to limiting warming under 1.5 °C by 2100 is to achieve a 45% reduction in human-caused CO_2 emissions by 2030 and to reach net-zero emissions by 2050 [2]. While the majority of GHG emissions reductions are expected to come from the implementation of clean renewable energy and changes to major carbon-emitting industries, a number of essential sectors lack a clear pathway towards net-zero emissions. These hard-to-abate sectors make up nearly 30% of global GHG emissions and include the manufacturing of essential chemicals and materials like cement, steel, aluminum and fertilizers, as well as heavy duty transportation industries including shipping, trucking and aviation [3]. The National Academy of Sciences released a report in 2019 describing a number of existing technologies that need to be adopted to meet short-term climate goals. Through a combination of soil conservation

* Corresponding author.
E-mail address: smcdaniel@reactivesurfaces.com (S. McDaniel).
[1] Dual first author.

https://doi.org/10.1016/j.jcou.2023.102421
Received 14 November 2022; Received in revised form 26 January 2023; Accepted 1 February 2023

practices, increased forest management efforts, biomass capture, processing, and distribution and other negative emissions technologies, it may be possible to achieve 10 billion tonnes of CO_2 removal per year in the first half of the century [4]. In order to reach large-scale and long-term removal goals of 20 billion tonnes of CO_2 per year in the second half of the century, costlier and less developed technologies like Direct Air Carbon Capture and Storage (DACCS) will need to be adopted at unprecedented levels [5].

In order to achieve removal targets of $GtCO_2$ per year, DACCS technologies must undergo massive up-scaling, a difficult feat considering typical energy-technology scale-up rates grow by an order of magnitude per decade or at a 26% annual growth rate [5]. However, with substantial subsidies and growing investment from industry, the scale-up rates required (45% annual growth) are not unheard of, with solar PV being a prime example [5]. Currently, two types of DAC technologies are on track to reach the required scales to meet climate goals: chemical liquid solvent DACCS systems (i.e., Carbon Engineering [6]) and chemical solid sorbent DACCS systems (i.e., Climeworks [7] and Global Thermostat [8]). Whether using a liquid or a solid substrate, the governing principles are the same; CO_2 from ambient air is fixed in the chemical liquid solvent or chemical solid sorbent with a chemical bond and then released as a high-purity CO_2 stream through the application of heat. The purified CO_2 stream must then be compressed, cooled, transported and injected into an underground CO_2 storage reservoir to achieve permanent sequestration. While chemical liquid solvent systems often require high-quality heat at 900 °C to separate the CO_2 from the solvent, chemical solid sorbent systems only require heat at 100 °C for the separation process, thereby enabling co-location with a number of industrial processes producing waste heat [5]. Synergistic placement of solid sorbent DACCS systems with geothermal or nuclear power plants would utilize low-carbon waste heat or use an industrial slip stream to provide 80% of the total energy demand for the system. The remaining 20% of the total energy demand is primarily for fans to move air through the system and is typically supplied by the local grid or from on-site renewable energy generation.

Several recent studies have evaluated the economic and environmental performance of chemical sorbent DACCS systems currently operating at commercial scales. Several common metrics are used to quantify the economic performance of DACCS systems: $ per tCO_2 captured, $ per tCO_2 net-delivered, and $ per tCO_2 net-sequestered. The first metric, $ per tCO_2 captured, quantifies the cost to operate the system long enough to remove or capture 1 tonne of CO_2 from ambient air. The second metric, $ per tCO_2 net-delivered, considers the direct GHG emissions from the system during the capture process and represents the cost to operate the system long enough to achieve a net removal of 1 tonne of CO2 from the atmosphere. The third metric, $ per tCO_2 net-sequestered, incorporates the GHG emissions and costs of compressing, cooling, transporting, injecting, and storing the CO_2 stream and represents the cost to achieve a net removal and durable sequestration of 1 tonne of CO_2 from the atmosphere. For all three metrics, various economic assumptions and cash flow models can be used to incorporate the time value of money, depreciation, loan payments and taxes into final capture and sequestration metrics. A recent study from Deutz and Bardow [9] provides a comprehensive life cycle assessment (LCA) of low-temperature sorbent systems from Climeworks currently operating in Switzerland and Iceland and found that these plants are achieving carbon removal efficiencies of 85% and 93%, respectively. While the results from Deutz and Bardow [9] provide valuable insight on the environmental performance of the evaluated DACCS system and associated supply chains, their results exclude environmental impacts from the compression, injection and storage stages necessary to achieve durable long-term sequestration. To the authors knowledge, the only comprehensive LCA of low-temperature sorbent DACCS systems including the injection and storage stage is from Terlouw et al. [10]. This recent study quantifies the impacts of utilizing various sources of heat (i.e., waste heat, electricity, and solar heat) and electricity (i.e., solar PV and grid energy) with Climeworks' low-temperature sorbent technology across a total of eight different locations. Of all the evaluated scenarios, carbon removal efficiencies range from 9% (high temperature heat pump and grid energy in Greece) to 97% (waste heat and grid energy in Norway) indicating a considerable dependence on low-carbon heat and energy to achieve desirable carbon removal efficiencies [10]. Another recent study from McQueen et al. [5] offers a robust techno-economic analysis (TEA) of Climeworks' low-temperature sorbent system when using natural gas, geothermal brine and a nuclear power plant slip stream as heat sources. For each of these sources respectively, McQueen et al. [5] report carbon removal efficiencies of 35%, 71%, and 71% and capture costs of $223, $205 and $233 per tCO_2 (and therefore capture costs accounting for removal efficiencies are $637, $288, and $328 per tCO_2 net-delivered) [5]. It should be noted, however, that the system boundary used by McQueen et al. [5] stops at compressed CO_2 delivery for use or storage and excludes actual injection into underground reservoirs. Regardless of the source of heat, the capture costs estimated by McQueen et al. [5] when using low-temperature sorbents are approximately $200 per tCO_2 captured. To understand the impact of including injection and storage in the system boundary, we can combine a baseline capture cost of $200 per tCO_2 with the range of carbon removal efficiencies reported by Terlouw et al. [10]. This suggests a potential range of $206 to $2222 per tCO_2 net-sequestered for solid sorbent technologies, highlighting the necessity to obtain low-carbon sources of heat and electricity for the capture and separation processes. Additionally, the need for low-carbon heat and electricity limits the scalability of low-temperature sorbent technologies by necessitating co-location with waste heat. Additionally, concerns exist regarding land use change when considering electricity generation using solar PV. Terlouw et al. [10] estimated land requirements as high as 4.7 km^2 for a solar PV system capable of supplying energy for DACCS plant with a capacity of 100 $ktCO_2$ per yr.

In addition to low-temperature sorbent systems, existing literature studies have evaluated the economic performance of high temperature chemical solvent DACCS technologies. In a study from 2018, Keith et a. [11] provide a robust TEA evaluating the technology used by Carbon Engineering and found that the baseline system with Nth plant economic assumptions was capable of capturing CO_2 from the atmosphere in the range of $126 to $170 per tCO_2 captured depending on the assumed capital recovery factor (7.5–12%). While the analysis lacks a comprehensive LCA, the preliminary LCA performed in the study estimates a carbon removal efficiency of 90% when using natural gas combustion with emissions recovery as the primary source of energy. When combined with the cost of capture, this yields a range of $140 to $189 per tCO_2 net-delivered for the chemical solvent DAC technology from Carbon Engineering. While the costs reported by Keith et al. [11] show favorable economic performance over low-temperature sorbent systems, high levels of uncertainty exist in economic results without a comprehensive LCA examining the system and quantifying all sources of re-emission. Additionally, while chemical solvent systems allow for centralized re-generation units and can achieve economies of scale, highly complex and costly infrastructure and the potential for a large water footprint provide potential obstacles in up-scaling to meet climate goals.

While decades of research and development have focused on the advancement of chemical solvent and sorbent technologies for DACCS systems, this study aims to assess a novel and emerging technology which exploits the biological process of photosynthesis to perform direct air capture on a large scale. The cultivation of microalgae for food and renewable fuels has been a research focus for biologists and engineers alike. Impressive photosynthetic rates drive high biomass yields per area and remove carbon from the atmosphere while producing a high value feedstock containing carbohydrates, lipids and proteins [12]. The composition of microalgae allows for a variety of high value co-products and can be made into renewable transportation fuels through a number of conversion processes including transesterification and hydrothermal

liquefaction [13]. This work exploits the fixation of carbon from the atmosphere in bacterial cellulose to perform direct air capture. When natural, carbon-fixing and polymerization genes from *Gluconacetobacter hansenii* (ATCC 53582, formerly *Gluconacetobacter xylinus*) are transfected into algal cells, the resulting recombinant algal cells can generate extracellular bacterial cellulose [14,15]. Similar engineered strains, when placed under growth-arrested conditions, have been shown to divert > 80% of biomass to photobiological production of compounds such as sucrose [16]. This work assumes the potential that algae under growth-arrested conditions over long terms effectively divert all biomass to the production of cellulose. Though incidental, significant algae cell replication outside growth-arrested conditions may increase the required nutrient content of the coating. Accumulation of cellulose in the coatings is approximated by experimental data for the growth of *Chlorella* on coated sheets. This approximation is corroborated by previous work showing engineered algal cells under arresting-growth condition to have increased carbon pulldown rates compared to wild-type cells [16].

In this study, we evaluate the carbon capture potential of a coated surface made from hydrogel, microalgae, nutrients and water. The coated surface, housed in a modular enclosure, has been designed to mimic the biological processes of lichens, by converting atmospheric CO_2 into bacterial cellulose which builds up on the surface over time. The coating is then harvested, and the constituents are separated with a chelator, allowing the generated cellulose to be converted to biochar through pyrolysis. The biochar is then land applied, providing an environmental service while durably sequestering the embodied carbon. While still in the early stages of development, there are many predicted advantages of this novel technology including the ability to quickly reach large-scale carbon removal using non-arable land. Additionally, once the initial surface has been seeded and deployed, the system is designed to remove carbon from the atmosphere and accumulate cellulose for months to years with minimal system inputs or required maintenance. The potential long operational life of this biomimetic surface would allow for rapid large-scale deployment across the globe. While the specific longevities of the algal cultures contained in the coating are currently being evaluated through lab-scale experiments, the economic and environmental impacts of this parameter are captured by modeling coating lifetimes of 1 year, 2.5 year, and 5 years in conservative, baseline and optimistic scenarios, respectively. Using these scenarios, this study aims to quantify the near-term environmental and economic performance of this novel carbon capture coating using a robust systems-level modeling approach, which serves as the foundation for integrated TEA and LCA with sensitivity and scenario analyses.

2. Materials and methods

2.1. System boundary

The system boundary of this study is drawn to ensure proper evaluation of the carbon removal efficiency and to allow a direct comparison to alternative DACCS technologies. While some studies truncate the system boundary at the delivery of purified compressed CO_2 [5] and suggest that industrial use of CO_2 from DACCS could assist in development and scaling of the technology, this study focuses on the goal of durable long-term sequestration. Thus, the system boundary of the study encompasses all upstream and downstream activities—including materials acquisition and emissions embodied in the modules and coatings, as well as emissions from operational energy, material replacement, maintenance, direct emissions to air from pyrolysis, and waste management at the end-of-life stage. A detailed process flow diagram is presented in Fig. 1, illustrating the system boundary and the mass and energy flows included in the system engineering model.

2.2. Functional unit

Existing TEA and LCA studies of carbon dioxide removal (CDR) technologies ([5,10,11]) report system performance using several different metrics including $ per tCO_2 captured, $ per tCO_2 net-delivered, $ per tCO_2 net-sequestered, as well as the overall carbon removal efficiency. This study uses an integrated approach to understand the net carbon removal of the coated surface technology using LCA methodology to account for atmospheric CO_2 removal and all sources of re-emissions within the system followed by a quantification of removal costs using TEA methodology. Thus, the functional unit of this analysis is the net total amount of carbon sequestered as determined through life cycle accounting. Economic results of the study are defined as the cost of carbon sequestration in $ per tCO_2 net-sequestered. This is determined by Eq. (1),

$$\frac{\$}{tCO_2\ net\ sequestered} = \frac{\$}{tCO_2\ captured} \Big/ \left(1 - \frac{tCO_2 emitted}{tCO_2 captured}\right) \quad (1)$$

where tCO_2 captured is the total amount of carbon dioxide (in metric tonnes CO_2) that is removed from the atmosphere by the system and tCO_2 emitted is the total carbon dioxide equivalent emissions (in metric tonnes CO_2-eq) directly or indirectly emitted by the system during the capture process.

2.3. Process model development

The carbon capture and sequestration process evaluated in this study is divided into four major sub-processes including coating manufacture and module construction, rotogravure printing, harvesting and separation and pyrolysis (Fig. 1). After printing, the coating is left protected in the enclosure with minimal maintenance over the course of its lifetime. Upon harvesting, the coating constituents are separated with chelating agents, the accumulated cellulose is charred for stable sequestration and the coating substrate is re-used for the production of new coated sheets. Conceptual illustrations of the proposed system are provided in the

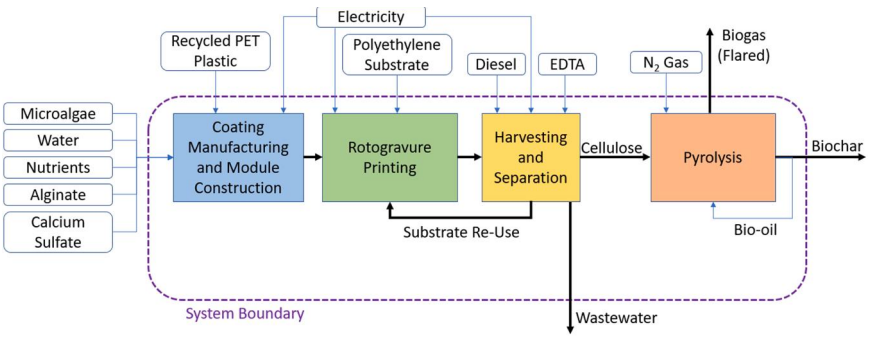

Fig. 1. Process flow diagram showing the system boundary and the material and energy inputs and outputs accounted for in the system engineering model and subsequent techno-economic and life cycle assessments.

Supplementary Information.

2.3.1. Coating manufacturing and module construction

The coating analyzed in this study consists of water (97% w/w), microalgae (0.09% w/w), alginate (1.29% w/w), calcium sulfate (1.38% w/w), tetrasodium pyrophosphate (0.09% w/w), and BG-11 nutrient formula (0.15% w/w). The coating is analogous to the other polymerized algae concepts [14,17–19]. Critical to the design of the carbon capture coating is the ability to reversibly polymerize and de-polymerize the polymer matrix. This is accomplished by using ionically polymerized hydrogels like alginate—that are unlike more widely-used covalently bonded coating polymers—and substituting strongly-bound calcium ions for weakly-bound sodium [14,20,21]. The coating architecture is depicted in Fig. 2. Once the cellulose is released from the hydrogel, the carbon in the cellulose can be converted into a form of durably-sequestered carbon such as biochar.

Initial algal cultures are obtained from commercial algae cultivation centers, or similar facilities to be built on site. These initial cultures are amplified to a dense inoculum level and combined with hydrogel-coating monomers, micronutrients, a calcium solution, and polymerization retardants to formulate the coating just prior to applying the formula to a polyethylene substrate using a rotogravure printing machine. After allowing a short time for the coating to cure, coated sheets are rolled into spools, transported, and installed in the modules using an integrated roller system. The total coated surface area of sheets installed in each module is determined by the maximum amount of carbon fixation based on the available quantity of incident solar radiation and carbon pulldown rate of the coating. Maximum carbon fixation, available solar radiation, and additional system constraints are discussed in detail in subsequent sections.

The coated sheets are protected from the environment by a transparent, open-air, modular enclosure made of recycled PET plastic. In essence the enclosure acts as a miniature green house that minimizes empty space and allows for modular deployment of the system. The modules are designed to achieve ample gas exchange and the passage of light energy required to sustain the algal cultures in the coating. While a number of more sophisticated module designs are currently being tested, this study assumes the use of a basic module with a built-in network of tensioned rollers arranged in a serpentine fashion, allowing rapid installation and harvesting of coated sheets at the end of their functional life. Conceptual illustrations of the proposed module are provided in the Supplementary Information. Strategic facility siting in warm and humid regions eliminates the need for module air conditioning and ensures temperatures and relative humidity remain within acceptable ranges. To achieve midcentury carbon removal goals, the system will have to be developed to operate in arid regions with higher evaporation, lower relative humidity, and high rates of solar radiation. Successful long-term deployment in arid regions will be met with additional challenges surrounding climate control, water retention, nutrient retention, and allowing air exchange within the modules while simultaneously attempting to limit water loss. Each module is 10 m long by 1 m wide by 1.5 m high with a wall thickness of 10 mm.

2.3.2. Rotogravure printing

Rotary printing presses, which can be calibrated for use in many applications, deposit the coating onto both sides of large, 0.8 m-wide sheets of woven polyethylene substrate at a deposition weight of 3.8 kg m^{-2} [22,23]. Following printing, the coated sheets are rolled into spools for transport and installation in the modular housings. Energy consumption for the rotogravure printing process was determined from an interview with an industry expert and was assessed at 0.6 kJ m^{-2} based on a 15-kW machine operating with a 1500 m^2 min^{-1} printing capacity.

2.3.3. Harvesting, separation, and drying

The sheets are rolled out of the coating housing using a forklift attachment and are loaded onto a flatbed trailer for transport to a centralized processing facility. The mean transportation distance was calculated assuming a circular facility layout with the processing facilities in the center, making the mean round trip transportation distance equal to the radius of the facility. At the time of harvesting, the coatings have amassed cellulose in proportion to deployment time. Benchtop laboratory experiments have already shown that the coating is still viable after > 1 month of deployment [14]. After 1 month of deployment, model outputs suggest the cellulose content has increased from 0% to 1.4% of the total coating mass through photosynthesis and cellulose accumulation. A majority of the remaining mass is water with less than 3% of total mass attributed to other coating materials in any case.

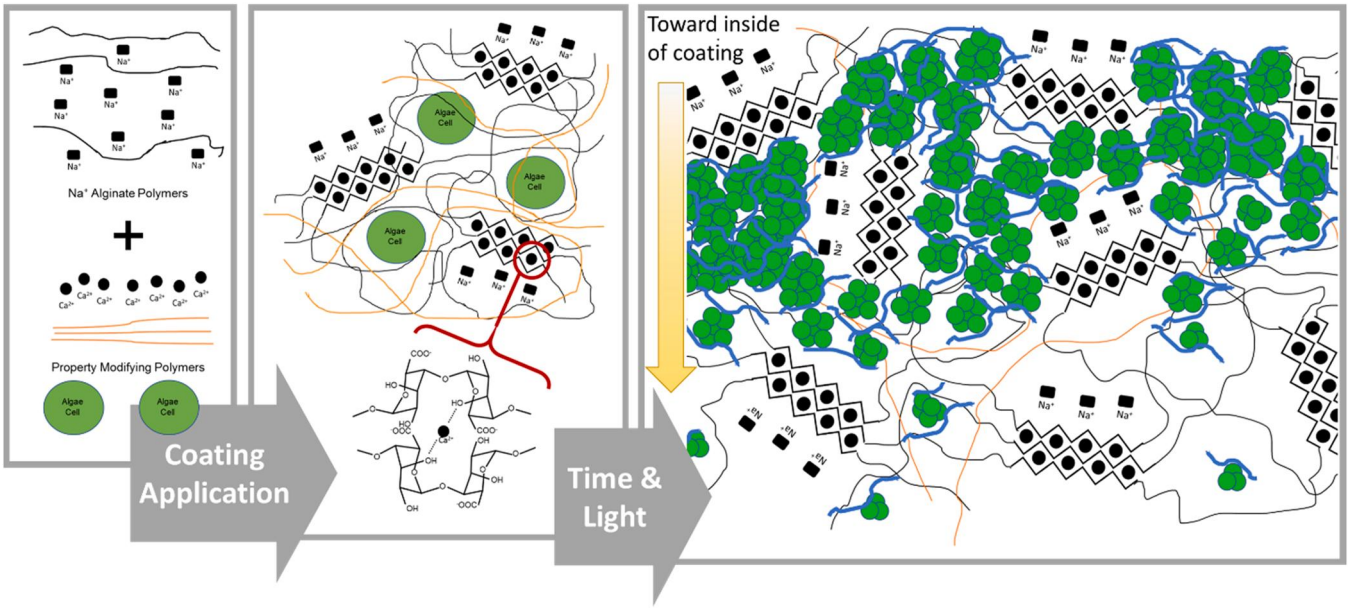

Fig. 2. Coating components and architecture showing increased cell density as the algae fix carbon dioxide during the photosynthetic process. Depending on the species of algae used, carbon is incorporated into cellular biomass (such as chitin and cellulose-like polysaccharides in the cell wall) or with genetically engineered strains, the cellulose can be excreted extracellularly (indicated by blue lines in the illustration).

The coating is stripped from the substrate using a chelating solution. The chelating step that disassociates the alginate polymers, micronutrients, algae biomass, and accumulated cellulose is achieved with metal chelators such as ethylenediamine tetra-acetic acid (EDTA). EDTA is a polyprotic acid containing four carboxylic acid groups and two amine groups with ion-pair electrons that ionically bond to calcium (and other metal ions). The process requires 0.078 kg sodium citrate kg^{-1} hydrated coating and 0.027 kg EDTA kg^{-1} hydrated coating. After disassociation of the alginate polymers, all the components of the coating formulation are soluble in water except cellulose [14]. If the suspended solids content of the stripped coating is less than 13% by weight, it is dewatered to 13% total suspended solids (TSS) via membrane filtration, followed by centrifugation to 20% TSS. If the chelated solution exceeds 13% TSS at the time of harvest, then the solution is sent directly to centrifugation to achieve 20% TSS. The supernatant from centrifugation is discarded and treated as industrial wastewater [24]. Membrane filtration and centrifugation are not required for the three main scenarios because the coating content is already greater than 20% TSS due to the accumulation of bacterial cellulose over the 1-month, 2.5-year, and 5-year growth periods respectively. Membrane filtration and centrifugation are similarly not required for some configurations during sensitivity and scenario analysis. The chelated solution is subsequently dried to 90% TSS with a drum dryer prior to pyrolysis [25]. Energy consumption for the membrane, centrifuge, and drum dryer were approximated as 0.4 kWh m^{-3} total flow, 1.35 kWh m^{-3} total flow, and 1.1 kWh kg^{-1} water removed, respectively [26,27]. Following the chelation and drying steps, the cellulose with 90% TSS is sent through pyrolysis and the polyethylene substrate can be reused and recoated with new coating formula.

2.3.4. Pyrolysis

Pyrolysis will occur at the centralized processing facility immediately following component separation. Pyrolysis is commonly used in the bio-energy sector to produce bio-oil, but a pyrolysis unit can be optimized for maximum biochar production with a coproduct of bio-oil by lowering the temperature and heat rate [28–32]. Phase yields and associated carbon streams for the conservative, baseline, and optimistic modeling scenarios are specified in Table 1. A low pyrolysis temperature of between 250 and 300 °C was assumed for maximum char production, while reaching an O/C atomic ratio below 0.6 [31,32]. Char with an O/C atomic ratio between 0.2 and 0.6 is considered stable for 100–1000 years [33]. At a temperature of 300 °C, an O/C atomic ratio of approximately 0.3 corresponds to approximately 71 wt% C when neglecting hydrogen, which makes up less than 5% of the total mass in this temperature range [31,32]. An output of 0.36 kg biochar/kg cellulose feedstock can be assumed at this temperature, resulting in 63% of the cellulosic carbon sequestered in the biochar product [31,32]. Bio-oil from the pyrolysis process was modeled as the fuel source for the pyrolysis heater. Assuming a LHV of 30 MJ/kg for the heavy oil, heater efficiency of 90%, heavy-oil output of 0.12 kg/kg feedstock [32], and pyrolysis energy demand of 0.27 kWh/kg feedstock [25], combustion of the heavy-oil fraction provided enough energy to meet 87%, 100%, and 100% of the total energy demand to dry and pyrolyze the coating material in the conservative, baseline, and optimistic scenarios respectively. This is a conservative estimate and additional energy can be provided through the combustion of the light oil fraction (0.4 kg/kg feedstock [32]) and heat recovery from the pyrolysis gas phase (0.11 kg/kg feedstock [32]).

2.4. Carbon capture coating performance

Since the algae in the coating fix atmospheric CO_2 into cellulose through photosynthesis, the major limiting factors in the coating's carbon removal rate are the total amount of incident solar radiation in the location of deployment and the photosynthetic efficiency of the microalgae. Calculations to determine the solar energy demand per kg of atmospheric CO_2 fixed into cellulose are based on the algae growth model developed by Greene et al. [12]. Estimation of the energy demand begins with the following chemical reaction representative of the photosynthetic process:

$$CO_2 + H_2O + (8 \sim 10\ Photons) \leftrightarrow CH_2OXX + O_2 \tag{2}$$

This assumed value of 8–10 photons per CH_2OXX represents the theoretical minimum for idealized systems and does not incorporate real-world losses [12]. Thus, the solar energy demand required to fix 1 kg of atmospheric CO_2 via photosynthesis, $E_{C_{fixation}}$, was derived with the following equation based on the methodology of Weyer et al. [34]:

$$\left(\frac{1 molCO_2}{0.044 kgCO_2}\right) * \left(8\frac{molPhotons}{molCO_2}\right) * \left(0.2253\frac{MJ}{molPhotons}\right) * \frac{1}{\varepsilon_T} * \frac{1}{\varepsilon_U} = E_{C_{fixation}}\frac{MJ}{kgCO_2} \tag{3}$$

In Eq. (3), the photon energy of 0.2253 MJ mol^{-1} photon was obtained from Weyer et al. [34] and corresponds to an average wavelength of 531 nm. This term represents the wavelength-weighted average photon energy within the portion of the solar spectrum utilizable for

Table 1
Critical modeling assumptions defined for the conservative, baseline, and optimistic scenarios. All parameters and values are representative of an 11,600-acre removal facility.

Parameter	Units	Optimistic	Baseline	Conservative	Ref.
Facility Size/Configuration					
Total Facility Size	acres	11,600	11,600	11,600	Calculation
Packing Density	m^2 surface/m^2 footprint	17	21	28	Calculation
Net CO_2 removal	tCO_2 sequestered/yr	921,000	896,000	805,000	Calculation
Physical Constraints					
Algae:					
Photon Transmission Efficiency	%	90%	90%	90%	[34]
Photon Utilization Efficiency	%	65%	65%	65%	[34]
Solar Energy:					
Full-spectrum Solar Energy	MJ m^{-2} $year^{-1}$	6573	6573	6573	[35]
Design Parameters					
Facility Operation:					
Operating Days	days	330	330	330	Assumption
Time to Harvest	years or months	5 years	2.5 year	1 year	Assumption
Coating Design/Performance:					
Carbon Removal Rate	mmol CO_2 m^{-2} hr^{-1}	12.5	10	7.5	Assumption
Pyrolysis Performance:					
Cellulosic Carbon to Biochar	%	63%	63%	63%	[31,32]
Cellulosic Carbon to Bio-oil	%	15%	15%	15%	[31,32]
Cellulosic Carbon to Bio-vapors	%	22%	22%	22%	[31]

photosynthesis (also called photosynthetically active radiation [PAR]). In Eq. (3), ε_T represents the photon transmission efficiency to account for a portion of the incident radiation that is reflected and absorbed by the transparent enclosure housing the coated surface, and ε_U is the photon utilization efficiency to account for the fraction of incident energy that is absorbed, but cannot be productively utilized (e.g., re-emitted as heat). Regionally-resolved estimates of Global Horizontal Irradiance (GHI) in kWh/m^2 were obtained from Solargis [35] and converted to PAR by assuming 45.8% of solar irradiance lies in the photosynthetic spectrum [34]. Geometric constrains allowing, maximum solar energy utilization in the Gulf Coast of the United States (where the mean horizontal irradiance is 6573 MJ m^{-2} yr^{-1} [35]) would yield an aerial productivity of 69 g DW cellulose m^{-2} day^{-1}.

To maximize carbon pulldown by the system and minimize costs, the surface area of coating per m^2 of ground area (packing density) was optimized. Eqs. (3) and (4) govern the theoretical maximum carbon pulldown by the system per square meter of facility aerial footprint.

$$CO_{2\max}\left(\frac{kgCO_2}{m^2\mathrm{s}}\right) = \frac{GHI\left(\frac{MW}{m^2}\right)}{E_{C_{fixation}}\left(\frac{MJ}{kgCO_2}\right)} = constant \tag{4}$$

Eq. (5) optimizes the packing density to minimize material requirements.

$$PD_{\min}\left(\frac{m^2_{\ coatedsurface}}{m^2_{\ aerialfootprint}}\right) = \frac{CO_{2\max}\left(\frac{kgCO_2}{m^2_{\ \text{aerial footprint}}}\right)}{\dot{R}_{pulldown}\left(\frac{kgCO_2}{m^2_{\ coatedsurface}}\right)} \tag{5}$$

Since the maximum carbon pulldown per m^2 of ground area is ultimately limited by the total amount of incident solar energy (Eq. (4)), the minimum surface packing density for the full utilization of solar energy, $PD_{\min}$, and the carbon pulldown rate of the coating, $\dot{R}_{pulldown}$(mmol CO$_2$ m^{-2} hr^{-1} or kg CO$_2$ m^{-2} s^{-1}), are inversely proportional (Eq. (5)). Lab-scale experiments have demonstrated carbon pulldown rates ranging from 5 to 10 mmol CO$_2$ m^{-2} hr^{-1} with the current coating formula, Fig. 3.

Pulldown rates are then calculated using the slope of the experimental data (see Supplementary Information). The pulldown rate starts at 10 and slowly decreased to less than 2 due to the concentration of CO$_2$ decreasing and the system being closed for measurement purposes. In a commercial system there would be a continuous flow of air and thus the CO$_2$ concentration would stay constant to support the higher pulldown rate.

The realistic maximum packing density is dependent on geometric constraints and potential issues with self-shading between coated sheets. Benchtop laboratory experiments have demonstrated packing densities within the module up to 11.2 m^2 per m^2 footprint. In comparison, the conservative, baseline, and optimistic scenarios assume carbon pulldown rates of 7.5, 10, and 12.5 mmol CO$_2$ m^{-2} hr^{-1} and would require minimum packing densities of 28, 21, and 17 m^2 per m^2 aerial footprint, respectively.

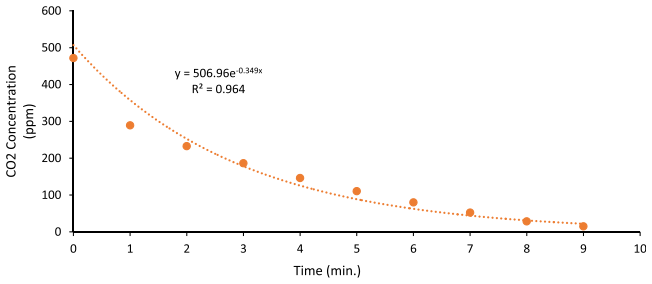

Fig. 3. Data from benchtop painted substrate testing. 30 L volume and surround lighting, with side light bias (PAR range of 55–380 μMol m^{-2} s^{-1}). Painted surface area to volume ratio of 48.33 m^2 m^{-3}. Data was collected by isolating the 30 L volume and monitoring CO$_2$ ppm for 9 min.

Optimizing the carbon pulldown rate of the coating ($\dot{R}_{pulldown}$) depends on the spacing between sheets of coated substrate, to avoid light-energy losses from self-shading. The minimum surface packing density for complete solar energy utilization increases as the carbon pulldown rate decreases, and high packing densities may be difficult to achieve without overexposing some sheets while shading others. With the carbon pulldown rate and packing density defined, the actual CO$_2$ pulldown per m^2 of ground area is determined using Eq. (6).

$$\begin{aligned} &if\ \ PD\left(\frac{m^2}{m^2}\right) < PD_{\min}\left(\frac{m^2}{m^2}\right)\ \ than\ \ CO_{2uptake} = \dot{R}_{uptake}\left(\frac{kgCO_2}{m^2\mathrm{s}}\right) * PD\left(\frac{m^2}{m^2}\right) \\ &if\ \ PD\left(\frac{m^2}{m^2}\right) \geq PD_{\min}\left(\frac{m^2}{m^2}\right)\ \ than\ \ CO_{2uptake} = CO_{2\max}\left(\frac{kgCO_2}{m^2\mathrm{s}}\right) \end{aligned} \tag{6}$$

Achieving maximum packing density while allowing full utilization of incident solar radiation represents a significant design hurdle that must be further addressed through innovative engineering and pilot-scale testing.

2.5. Modeled scenarios and critical assumptions

All results presented in this study are for a facility with a fixed size of 11,600 acres. Total net carbon removal, total capital, and total operational expenses are dependent on a number of critical assumptions. The facility was modeled in the Gulf Coast region of the United States of America where the mean horizontal irradiance is 6573 MJ m^{-2} yr^{-1} [35]. Modules housing the carbon capture coatings cover 75% of the facility footprint, and a road network for coating harvest in addition to centralized coating production and pyrolysis facilities occupy the remaining space. Three scenarios (conservative, baseline, and optimistic) were developed to capture the possible range in costs and carbon removal efficiencies of the system. Only the carbon pulldown rate and time to harvest were varied between the three scenarios as these variables represent the largest source of uncertainty in the analysis and directly impact net carbon removal and system costs. The critical parameters and assumed values for each of the modeled scenarios are presented in Table 1.

While the water-retaining characteristics of the coating were assumed to eliminate the need for makeup water, water loss through evaporation is still expected to occur. Annual water losses (expressed as a percentage of the initial water retained in the coating) were defined for each modeling scenario and are presented in Table 1. Water loss from evaporation is only assumed to impact the solids content of the coating at the time of harvest, and well water was assumed to be used for the production of new coating formula following each harvesting event.

2.6. Capital expenses

Capital costs were quantified for all components of the system including the purchasing and preparation of land, manufacturing of coating constituents and housings, and equipment for deployment, maintenance, harvesting, separation, and pyrolysis. Capital costs were referenced from literature and adjusted to the suitable capacity using a scaling parameter and exponent where appropriate. The chemical engineering plant cost index (CEPCI) was used to bring all referenced costs to 2019 dollars [36]. Capital cost assumptions are presented in Table 2.

The cost of the modular enclosures was quantified on a per m^2 basis and includes the cost of rollers to allow for rapid deployment and harvesting of coated surfaces. Greenhouse structures range in cost from $87 per m^2 to $128 per m^2 and provide the most direct comparison to the planned module housing [37]. The coating modules are assumed to be cheaper than standard greenhouse enclosures, as the snap-together components do not require a steel frame, utilize recycled PET material, contain minimal equipment overall, and can be mass produced with an assembly line.

Table 2
Total capital cost of major equipment for an 11,600-acre facility (conservative Scenario).

Major Capital Expenses	Unit Cost	Capacity	Cost	Cost Year	Ref.
Recycled PET Modules	$50/m^2 footprint	-	$2,341MM	2019 USD	[37]
Rotogravure Printing Machines	$160 K/ printer	1257 m^2/ min	$0.31MM	2019 USD	[38]
Forklifts	$30 K/ forklift	-	$0.926MM	2019 USD	[39]
Flatbed Semis	$100 K/ semi	-	$6.20MM	2019 USD	[40]
Separation/ Chelating Units	$160 K/ printer	1257 m^2/ min	$0.31MM	2019 USD	Estimate
Pyrolysis Units	$62MM/ unit	775 tonne/ day	$249MM	2019 USD	[25]
Membrane[a]	$10.4MM/ unit	13.4 MGD	n/a[a]	2019 USD	[26]
Centrifuge[b]	$2.7MM/ unit	211 m^3/hr	n/a[a]	2019 USD	[26]
Drum Dryer	$329 K/ unit	1000 kg water evaporated/ hr	$43.8MM	2019 USD	[24]

[a] Required only if % solids is less than 13%.
[b] Required only if % solids is less than 20%.

The full-scale facility is constructed incrementally. For example, with a grow-out period of 5 years between harvests, 1/5th of the facility is opened annually over 5 years. An initial investment of coating materials and substrate for 1/5th of the total facility footprint is incurred each year for the first 5 years of operation. The first harvest takes place in year 6, when all coated surfaces from year one are collected, separated, sent through pyrolysis, and land applied. From this year forward the facility operates in a continuous fashion, harvesting 20% of the total acreage annually. For growth periods of 1 year, 2.5 years, and 5 years, the facility would harvest 32, 13, and 6.4 acres per day, respectively. Running the facility in this manner reduces the burden on printing, processing, and minimizes the required pyrolysis capacity. The cost for printing was determined from an interview with an industry expert. The facility would require 2, 1, and 1 high-speed printing machines with printing capacities of 1300, 800, and 300 m^2 min^{-1} for the conservative, baseline, and optimistic scenarios, respectively.

Capital costs were quantified for equipment needed to harvest and transport coated surfaces from housing modules to the processing facility, as well as the equipment needed for coating separation and pyrolysis. For the 11,600-acre facility, two trucks and one forklift were included for every 500 acres of facility footprint for hauling. The cost of reclamation equipment was approximated as an additional rotogravure printer fitted with the equipment necessary to strip the coating from the substrate. The cost of a centrifuge and drum dyer were approximated from Davis et al. [26]. The cost of pyrolysis equipment including phase separation was adapted from previous work in the bio-energy sector [25]. The cost of a 41,667 kg hr^{-1} capacity pyrolysis unit including the combustor and downstream phase separation equipment was sourced from Dutta et al. [25] and scaled based on total calculated processing capacity using a scaling exponent of 0.8. Land was assumed to cost $3000 per acre, representative of low-value, non-arable land in the Gulf Coast of the United States [26]. Site development including land grading, office construction, and project contingency were assessed as a percentage of equipment and infrastructure costs based on the work of Davis et al. [26] and are outlined in Table 3.

Table 3
Additional direct and indirect capital costs for the system.

Other direct capital costs	**Pyrolysis, printing, and harvesting facilities CAPEX**	**Modular coating housings and initial carbon capture coating CAPEX**
Buildings	4%	1.20%
Site development	9%	Included above
Additional piping	5%	Included above
Indirect capital cost	**Pyrolysis, printing, and harvesting facilities CAPEX**	**Modular coating housings and initial carbon capture coating CAPEX**
Proratable expenses	10%	4%
Field expenses	10%	5%
Home Office Construction	20%	10%
Project Contingency	10%	10%
Other Costs	10%	3%

2.7. Operational expenses

2.7.1. Variable operational expenses

Variable operational costs include electricity for printing machines, water pumps, and pyrolysis conveyers, diesel for harvesting, nitrogen as an inert gas for pyrolysis, well water, and the various coating constituents necessary to re-surface the polyethylene substrate. Variable operational costs for the 11,600-acre facility are summarized in Table 4.

Nitrogen for pyrolysis was assumed to come from an onsite air separation unit. The modeling of this unit was considered outside the scope of the study and the cost of nitrogen listed in Table 4 represents the levelized cost of onsite nitrogen production. Annual water consumption for the system was calculated as 1320, 396, and 158 thousand m^3 per year based on the assumed coating replacement rates of 1 year, 2.5 years, and 5 years, respectively. The wastewater treatment cost was based on the total wastewater discharge with costs obtained from a 2002 survey of industrial and commercial wastewater treatment facilities, updated to 2019 dollars with the cost of clean water index [24,43].

2.7.2. Fixed operational expenses

Fixed operational expenses consist of labor and labor burdens, maintenance, and insurance. The rotogravure printing process in which the carbon capture coating is deposited on the substrate would require 5

Table 4
Major variable operational costs defined for an 11,600-acre facility.

Parameter	Units	Value	Ref.
Major Material Costs			
Utility Costs:			
Electricity (On-site Solar PV)	$/kWh	0.09	[41]
Natural Gas	$/1000 SCF	5.10	[26]
Diesel	$/gallon	3.03	[42]
Wastewater Processing Fee	$/1000 gallons	4.67	[24,43]
Coating Constituents:			
Polyethylene Substrate	$/m^2	0.18	[44]
Microalgae Biomass	$/tonne AFDW	1500	[45]
Other Constituents (listed below):	$/kg dry wt.	0.16	Assumption*
Alginate			
Calcium Sulfate			
Tetrasodium Pyrophosphate			
BG-11			
Chelating solution:			
Sodium Citrate	$/kg	0.50	[46]
EDTA	$/kg	0.70	[47]
Other Materials:			
Nitrogen	$/kg	0.16	[48]
Well Water	$/m^3	0.40	[26]
Biochar Selling Price	$/tonne	100	[49]

*Cost of "Other Constituents" based on current lab expenses with significant bulk discounts applied.

operators operating on a continuous, 24-hour schedule. Maintenance and management were assumed to be minimal from the moment the coatings have been deployed until they are harvested. 240 field laborers would be responsible for monitoring the coating modules and performing general maintenance tasks such as washing dust and debris from the coating housings, replacing damaged surfaces, and checking additional routine maintenance items. Each worker would manage roughly 48 acres of the facility.

Harvesting is assumed to be a labor-intensive process. The 240 field laborers also serve as coating harvesters. For the conservative scenarios with a 1-year grow out between harvests, roughly 32 acres would be harvested daily. Teams of two laborers would be responsible for harvesting 107 modules daily by rolling up the surfaces into spools and staging them for collection along the service roads. Several collection teams equipped with forklifts and flatbed semi-trucks would drive along the service road, collecting the rolls and transporting them to the centralized processing facility. Once rolls of coated surfaces have arrived at the centralized processing facility, the separation process requires an additional 5 operators working rotating shifts to operate on a continuous 24-hour schedule. All required personnel for the 1 $MtCO_2$ per year facility are outlined in Table 5.

The facility capacity, as reflected in total operating days, accounts for maintenance of engineered equipment at the centralized facilities. While equipment is expected to need regular general maintenance, the coatings operate continuously from deployment until harvesting. Insurance and maintenance are assessed as 0.7% and 3% of total direct capital (TDC) expenses, respectively [26].

2.8. Techno-economic analysis methodology

The techno-economic analysis was performed using a 30-year discounted cash flow rate of return (DCFROR) model to determine the minimum cost of carbon removal in $ per tCO_2 net sequestered. A 7 year Modified Accelerated Cost Recovery System (MACRS) depreciation schedule was applied to the total equipment capital investment for all equipment including the pyrolysis system. The MACRS depreciation scheme was chosen to be consistent with existing TEA studies for numerous Nth scale bio-energy systems and to allow comparison of the results to alternative DACCS technologies. Furthermore, the cash flow model assumed a 10% internal rate of return (IRR), and an income tax rate of 35% over the 30-year time horizon for the economic analysis. The TEA assumed 40% equity, a loan term of 10 years, and an interest rate of 8%. The working capital was assumed to be 5% of the total system capital expenditure. Revenue generated from the biochar product was incorporated into the analysis to determine a minimum cost of carbon capture such that a net present value of zero was achieved based on an internal rate of return of 10%. Results are expressed with the metric USD per tonne of atmospheric CO_2 durably sequestered (i.e., 100 + years).

Table 5
Labor requirements for an 11,600-acre removal facility.

Parameter	Base Salary	Ref.
Labor Costs		
Facility manager	$73,613	[50]
Operations manager	$73,613	[50]
Operations specialist	$73,613	[50]
Coating machine operator	$42,900	[50]
Harvest supervisor	$73,613	[50]
Module/harvest laborer	$33,500	[50]
Pyrolysis operator	$42,900	[50]
Site engineer	$73,613	[50]
Pyrolysis engineer	$73,613	[50]
Maintenance specialist	$73,613	[50]
Labor Burdens	90% of Base Salary	[26]
Total Annual Labor Costs	**$16,475,288**	

2.9. Life cycle assessment

2.9.1. Methodology

This LCA study is attributional and operates under the assumption that the primary production of materials is allocated to the primary user and recycled materials are provided burden free to subsequent processes. LCI data were gathered, system boundaries were developed, and burdens and credits have been allocated in accordance with ISO 14040 standards [51]. All scope 1 and 2 operational emissions are accounted for. This project has a large upfront burden for manufacturing and assembling infrastructure with minimal operational emissions. Emissions associated with major infrastructure including the recycled PET modules and initial coating and substrate constituents were included in the system boundary, while emissions associated with the production of machinery including forklifts, semi-trucks, printing machines, and pyrolysis units were excluded from the system boundary and assumed to be negligible compared to emission for the initial coating material constituents, the coating substrate, and the modular coating housings due to the mass of the materials.

2.9.2. Life cycle inventory data

Lifecycle inventory (LCI) data was acquired directly from the Ecoinvent database (version 3.7) [52] whenever available. Materials acquisition and manufacturing of the PET coating housings was approximated using a surface area of 53 m^2 per module, a thickness of 10 mm, 405 modules per acre and assuming the use of extruded recycled polyethylene terephthalate (PET) plastic. Substrate material was modeled as polyester fiber made from recycled polyethylene granulate. The production of microalgae biomass and alginate were assumed to result in net-zero emissions based on the modeling work of Greene et al. [12]. Emissions for BG-11 were approximated using ammonia and DAP as a proxy, obtaining total required mass based on delivering equivalent nitrogen and phosphorous content to the coating.

2.10. Sensitivity and scenario analysis

Various sensitivity and scenario studies were performed to check model functionality and understand the influence of high-impact parameters on final results metrics. Model sensitivity was investigated by adjusting critical model inputs by ± 10% and recording the resulting change in the cost of carbon capture and sequestration. The tested model parameters were then ranked from most to least impactful to determine which modeling inputs should be subject to further sensitivity and scenario analysis. Several input variables were identified as being high impact and/or simultaneously carrying large uncertainty and these variables included the carbon pulldown rate, the time to harvest, and the module packing density. All three of these variables were subject to scenario analyses in which the selected variable was adjusted across a large range of possible values while recording the resulting change in the cost of carbon capture and sequestration.

3. Results

The results require integrated life cycle assessment with techno-economic modeling to determine the minimum cost of carbon capture and sequestration. A critical component of the work is accurate emissions accounting as both the direct and indirect emissions from the process must be considered. The results are divided into three sections and start with the minimum cost of carbon sequestration results followed by details on the life cycle assessment, and lastly results from sensitivity and scenario analyses.

3.1. Minimum cost of carbon sequestration

The total capital expenditure and annual operational expenses of the system were combined with the carbon removal efficiency to determine

the total capture and sequestration cost per tonne CO_2 net-sequestered based on a discounted cash flow rate of return analysis. After accounting for all sources of re-emission, the capture and sequestration cost shown in Fig. 4 represents the cost to transform 1 tonne of atmospheric CO_2 into biochar using a coated substrate system with a total facility footprint of 11,600 acres. Additionally, the results in Fig. 4 represent the minimum product selling price (MPSP) or the value of sequestered CO_2 that yields a 10% internal rate of return over the 30-year life of the plant.

The results in Fig. 4 suggest a total capture and sequestration cost of $1585, $822, and $702 per tonne CO_2 net sequestered for the conservative, baseline, and optimistic scenarios, respectively. The largest cost contributor for all scenarios is the recycled PET modules, which contributes $763, $466, and $423 to the minimum product selling price for the conservative, baseline, and optimistic scenarios, respectively. The results in Fig. 4 suggest the system is capitally intensive, and the total capital expenditure (shades of blue and green in Fig. 4) contribute 65%, 73%, and 75% to the minimum product selling price for the conservative, baseline, and optimistic scenarios, respectively. Maintenance costs are a function of the total capital expenditure and also contribute a large portion of the MPSP (13%, 15%, and 16% for the conservative, baseline, and optimistic scenarios, respectively). The carbon capture and sequestration cost for the optimistic scenario shown in Fig. 4 is on par with existing DACCS technologies such as Climeworks low temperature sorbent system (with natural gas as a heat source) with a reported capture cost of $637 per tonne CO_2 captured [5]. Furthermore, the capture and sequestration cost shown in Fig. 4 include all related costs to achieve durable sequestration in the form of biochar, while the costs reported by McQueen et al. [5] exclude injection of the compressed CO_2 stream into underground storage. The resulting capture and sequestration cost shown in Fig. 4 is heavily dependent on the carbon removal efficiency of the system. The carbon removal efficiency represents the total GHG emissions (in kg CO_2-equivalence) incurred from manufacturing facility infrastructure and operating the facility long enough to sequester 1 kg of atmospheric CO_2 in the form of biochar. Results for the carbon removal efficiency are presented in Fig. 5.

3.2. Carbon removal efficiency

The results in Fig. 5 suggest that for each kg of CO_2 captured from ambient air and converted to biochar, the system emits 0.73, 0.56 and 0.51 kg of CO_2-eq for the conservative, baseline, and optimistic scenarios, respectively. These system re-emissions result in capture efficiencies of 27%, 44%, and 49% for the conservative, baseline, and optimistic scenarios, respectively. Thus, the optimistic scenario with a capture efficiency of around 50%, the facility must remove 2 tonnes of CO_2 to achieve the net removal of 1 tonne of CO_2. The results in Fig. 5 suggest reemission during pyrolysis in the form of exhaust gas is a key driver for the carbon removal efficiency, emitting 0.37, kg CO_2-eq per kg CO_2 net sequestered in all scenarios. Further tailoring the pyrolysis equipment to maximize biochar could result in improvements to the overall carbon removal efficiency by reducing exhaust gas emissions and could reduce capture and sequestration costs. Despite using recycled PET plastic, the manufacturing of the coating modules provides the second largest source of system emissions, emitting ~0.07 kg CO_2-eq per kg CO_2 net sequestered across all three scenarios. Another large source of system emissions is the production of chelators used in the harvesting process, which results in an emission of 0.19, 0.06, and 0.02 kg CO_2-eq per kg CO_2 net sequestered for the conservative, baseline, and optimistic scenarios, respectively. Recycling chelating agents could reduce this impact but would add to system complexity. Another variable greatly

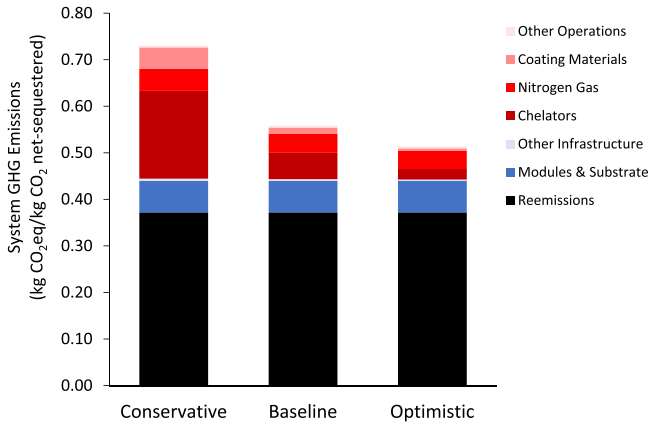

Fig. 5. Carbon removal efficiency utilizing the carbon capture coatings housed in modular enclosures. Results are representative of an 11,600-acre facility operating under conservative, baseline, and optimistic assumptions.

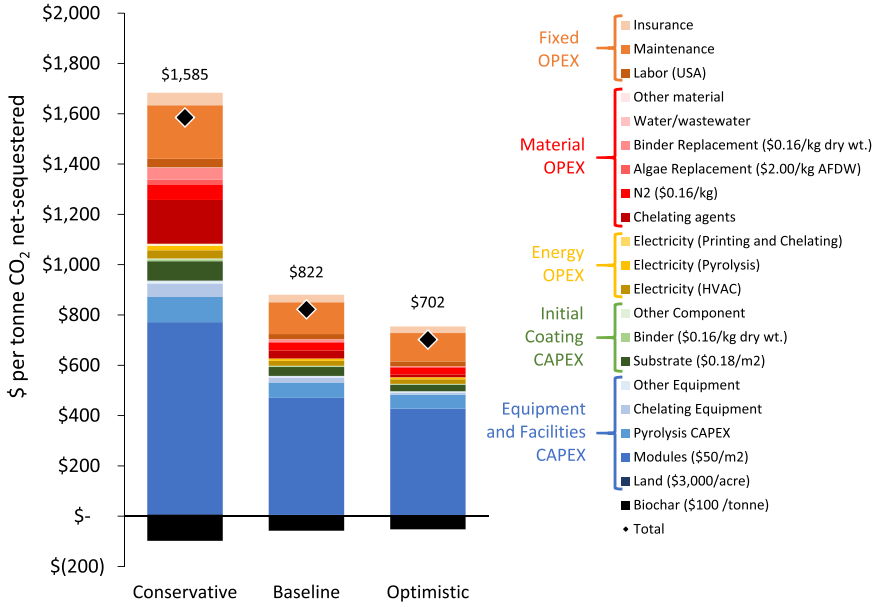

Fig. 4. Cost of CO_2 capture and sequestration (tCO_2$ net sequestered) utilizing the carbon capture coatings housed in modular enclosures. Results are representative of an 11,600-acre facility operating under conservative, baseline, and optimistic assumptions.

impacting the overall system capture efficiency is the time to harvest. For shorter harvesting periods, there are more harvesting events within the same time frame resulting in a larger quantity of required coating material replacements and chelating agents, resulting in larger system emissions. For example, the 1-year harvesting period assumed in the conservative scenario results in system emissions of 0.05 kg CO_2-eq per kg CO_2 net sequestered for the required coating replacement materials, whereas the 5-year harvesting period in the optimistic scenario results in system emissions of 0.005 kg CO_2-eq per kg CO_2 net sequestered embodied for the required coating replacement materials (a 90% reduction).

3.3. Sensitivity and scenario analyses

Several sensitivity and scenario analyses were performed to ensure model functionality and explore high impact variables. Modeling inputs were varied by ± 10% relative to the baseline assumptions while recording the resulting change in the total cost of carbon capture and sequestration. The results of the sensitivity analysis are shown in Fig. 6.

The results from the sensitivity analysis indicate that the model is most sensitive to the carbon pulldown rate and the harvest interval. These two parameters dictate the consumption of coating materials. The model is also sensitive to photon transmission efficiency, the portion of radiation that is PAR, the annual full-spectrum solar energy, photon utilization efficiency, the photon quantum requirement, and photon energy. Each of these variables dictate the theoretical maximum carbon uptake by the coated surfaces. The model is also impacted by the enclosure manufacturing cost, as it contributes 45–60% of the total capture and sequestration cost shown in Fig. 4. Lastly, the model is impacted by coating water content and chelator requirement because they dictate the consumption of chelating chemicals.

Several of the sensitive input variables carry a large amount of uncertainty, and scenario analyses were performed to understand the impact of adjusting these highly uncertain parameters. While lab experiments have demonstrated carbon pulldown rates that align with the assumptions of this study, one of the goals of modeling was to determine the point at which further increases to the pulldown rate result in diminishing returns. The carbon pulldown rate was varied from 1 to 20 mmol m^{-2} hr^{-1} while recording the carbon capture and sequestration cost of the system. Results in Fig. 7 show the impact of the pulldown rate for the conservative scenario.

Results from this scenario analysis show that the system will see diminishing returns when exceeding a carbon pulldown rate of about 10 mmol m^{-2} hr^{-1}. Below 5 mmol m^{-2} hr^{-1} the system sees an exponential increase in system costs and below 4 mmol m^{-2} hr^{-1} the system emits more CO_2 than is captured resulting in a capture and sequestration cost approaching infinity. The results from this scenario analysis indicate that 10 mmol m^{-2} hr^{-1} is a reasonable target within the range of experimentally demonstrated pulldown rates, above which the system will see diminishing returns. However, one benefit of achieving higher

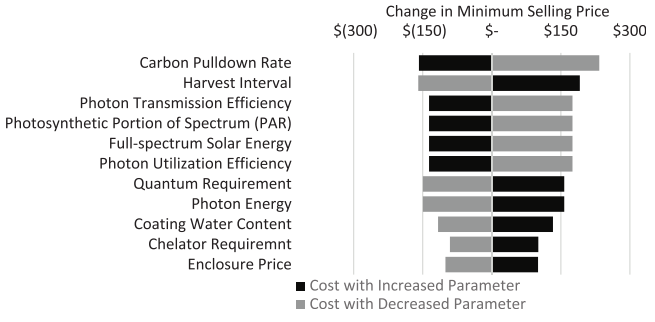

Fig. 6. Results from the sensitivity analysis in which modeling inputs were adjusted by ± 10% with the resulting impact recorded as the change in the minimum CO_2 selling price.

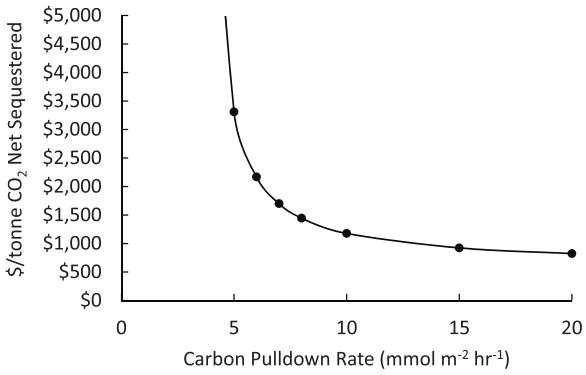

Fig. 7. Conservative scenario carbon pulldown rate vs. the cost of carbon capture and sequestration in $ per tonne CO_2 net-sequestered.

pulldown rates is the ability to spread sheets out within the module and maximize light utilization, which could eliminate potential problems with over-packing, self-shading, contamination, and air flow within the modules. These potential impacts are not quantified in the model, as the minimum packing density for maximum light utilization was calculated and assumed for each of the three modeled scenarios. In addition to the carbon pulldown rate, duration to harvest was subject to scenario analysis (Fig. 8) because, while open raceway ponds can sustain cultures for months to years without complete culture failure, the containment of genetically modified algal cultures on coated surfaces has yet to be demonstrated at scale for the lifetimes assumed in this modeling work. Lab-scale experiments have successfully sustained coated sheets for months without the addition of water, nutrients, or fungicides.

The results in Fig. 8 illustrate the impact of the harvesting interval, or the time between coated surface deployment and harvest, on the overall cost of capture and sequestration in $ per tonne CO_2 net-sequestered. The results suggest that there are costs and emissions incurred regardless of the assumed harvesting interval, which help to dictate the horizontal asymptotes in Fig. 8. For example, the PET modules must be built for the entire facility regardless of the harvesting interval. As such, as the harvesting interval is decreased, the system incurs additional costs and emissions, such as coating replacement and chelating agents that further increase the capture and sequestration costs, while the harvesting interval is decreased. The capture cost reaches vertical asymptotes approaching infinity as the harvesting interval is reduced below 3.7 months. With a harvesting interval shorter than 3.7 months, the required system materials and embodied emissions result in net CO_2 emissions and the cost of capture and sequestration approaches infinity. The results suggest that a minimum harvesting interval of 6–10 months is imperative to reach economic feasibility of capture and sequestration costs below $2000 per tonne CO_2 net-sequestered. Beyond a 24-month harvesting interval, however, the system sees diminishing returns. The last variable subject to scenario analysis was the packing density of coated surfaces within the modules. Geometric constraints within the module and the possibility of self-shading or light-attenuation from the PET material present a large source of uncertainty for the overall performance of the system. As shown in Fig. 9, packing density was adjusted from 0 to 30 m^2 per m^2 footprint to determine the impact on the cost of capture and sequestration.

For each curve in Fig. 9, the furthest point to the rights illustrates the lowest possible capture and sequestration cost for the given scenario and represents the lowest possible packing density to utilize all of the available solar radiation for carbon fixation via photosynthesis. Any further to the right (higher packing density) would result in an excess of coated materials within the module and with insufficient light availability (i.e., light-limited operation). Following the curve to the left results in an increase in system costs, because there is insufficient surface area to utilize all of the available solar energy, resulting in lower carbon

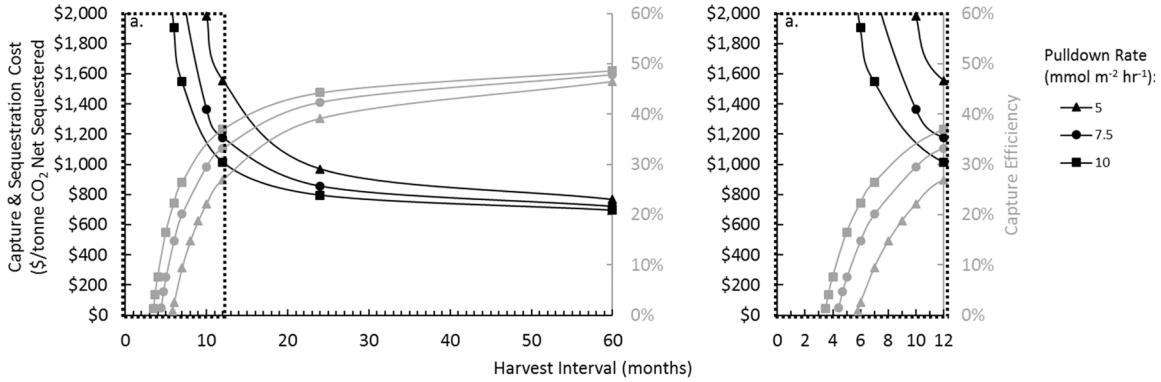

Fig. 8. Harvest interval (months) vs. the cost of carbon capture and sequestration in $/tonne CO_2 net-sequestered (black lines) and the overall capture efficiency (gray lines).

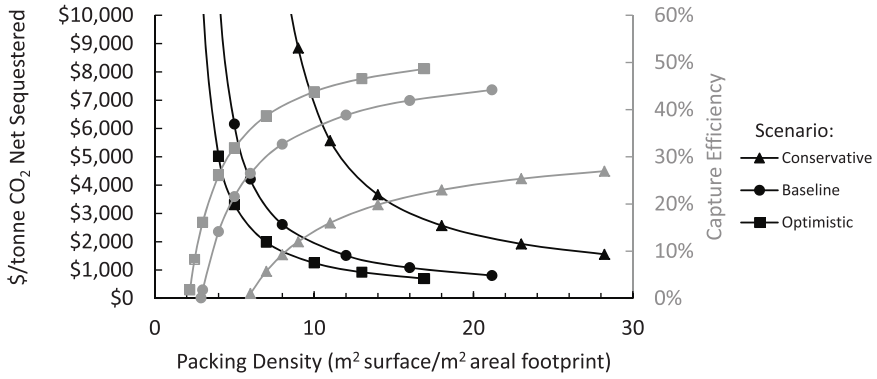

Fig. 9. Module packing density (m^2 coated surface per m^2 areal footprint) vs. the cost of carbon capture and sequestration in $ per tonne CO_2 net-sequestered.

capture per ground area (i.e., coating-limited operation). No matter the scenario, capture costs approach infinity as the packing density approaches 0 and a minimum packing density of 2.2 m^2 surface per m^2 footprint is required to achieve net carbon removal. If the packing density decreases below 2.2 m^2 surface per m^2 footprint, then the system emits more CO_2 than captured. Packing densities above 7–20 m^2 surface per m^2 footprint are required for system costs to remain below $2000 per tonne CO^2 net-sequestered and diminishing returns are seen around 7, 12, and 20 m^2 surface per m^2 footprint for the optimistic, baseline, and conservative scenarios, respectively. Achieving the optimal packing density without encountering geometric constraints or causing self-shading of surfaces within the modules and successfully demonstrating the optimal packing density will be a large milestone in the development of this proposed concept.

Harmonizing results for low-temperature sorbent systems from McQueen et al. and Terlouw et al. as described in the introduction, a potential range of $206 to $2222 per tCO_2 net-sequestered is determined for solid sorbent DAC technologies depending on carbon removal efficiency [5,10]. As illustrated in the scenario analyses, the coating lifetime must exceed 1.5 months with a packing density of 17 m^2 surface per m^2 footprint to results in net carbon removal and must exceed 3–4 months to achieve economic parity with these existing carbon capture systems. While these existing carbon capture systems can achieve greater than 90% carbon removal efficiency, the need for low-carbon heat and electricity limits the scalability of low-temperature sorbent technologies by necessitating co-location with waste heat or the new construction of on-site solar energy [9,10]. Carbon removal efficiency of these systems can be as low as 9% without co-location and with a non-renewable grid mix [10]. The process outlined in this report can achieve carbon removal efficiency of 51–73% without the necessity for co-location. Regardless of technology, utilizing solar energy through photovoltaics or algae has large land requirements. All direct air capture technologies require improvement and cost reduction to achieve the $17–$50 value in current (January 2021) emissions trading system markets or the $2.6–$140 price of current carbon taxes [53].

4. Conclusions

The analysis presented here provides a preliminary techno-economic analysis and life cycle assessment of a novel algae-based carbon capture coating. The results obtained from the analysis are representative of a large-scale facility capable of sequestering 1 million tonnes of atmospheric CO_2 per year in the form of biochar. Results from the analysis shows the system emits 0.27–0.49 kg CO_2-eq per kg CO_2 sequestered (73–51% carbon removal efficiency) and achieves a capture and sequestration cost of $702–$1585 per tonne CO_2 net sequestered. The capture costs estimated with this study are on par with existing DACCS technologies, including Climeworks' low-temperature sorbent system. Furthermore, the proposed technology offers rapid scale-up potential with the ability to utilize non-arable land and solar radiation for energy, factory line assembly of facility infrastructure, re-use of coating constituents and housings and long periods of minimal maintenance. System economics are expected to improve significantly through engineered solutions that reduce total capital expenditure, tailor the pyrolysis process to maximize biochar formation and maximize material recycling efficiencies within the system.

CRediT authorship contribution statement

Garrett M. Cole: Data curation, Formal analysis, Investigation, Methodology, Software, Validation, Visualization, Writing – original draft, Writing – review & editing. **Jonah M. Greene:** Data curation,

Formal analysis, Investigation, Methodology, Software, Validation, Visualization, Writing – original draft, Writing – review & editing. **Jason C. Quinn:** Funding acquisition, Investigation, Methodology, Project administration, Supervision, Writing – original draft, Writing – review & editing. **Beth McDaniel:** Conceptualization, Funding acquisition, Project administration, Writing – original draft, Writing – review & editing. **Lisa Kemp:** Data curation, Writing – review & editing. **David Simmons:** Data curation, Writing – original draft, Writing – review & editing. **Tyler Hodges:** Data curation, Writing – original draft, Writing – review & editing. **David Nobles:** Data curation, Writing – original draft, Writing – review & editing. **Taylor Weiss:** Data curation, Writing – original draft, Writing – review & editing. **John McGowen:** Data curation, Writing – original draft, Writing – review & editing. **Steve McDaniel:** Conceptualization, Funding acquisition, Project administration, Writing – original draft, Writing – review & editing.

Declaration of Competing Interest

The authors declare that they have no known competing financial interests or personal relationships that could have appeared to influence the work reported in this paper.

Data availability

Data will be made available on request.

Acknowledgments

The authors acknowledge funding for the work from Reactive Surfaces to Sustainability Science.

Appendix A. Supplementary material

Supplementary data associated with this article can be found in the online version at doi:10.1016/j.jcou.2023.102421.

References

[1] Climate Change Evidence: How Do We Know? Climate Change: Vital Signs of the Planet. ⟨https://climate.nasa.gov/evidence⟩, (Accessed 26 July 2021).
[2] Summary for Policymakers of IPCC Special Report on Global Warming of 1.5°C approved by governments — IPCC. ⟨https://www.ipcc.ch/2018/10/08/summary-for-policymakers-of-ipcc-special-report-on-global-warming-of-1-5c-approved-by-governments/⟩, (Accessed 26 July 2021).
[3] Tackling the Harder-to-abate Sectors: Join the Conversation, World Economic Forum. ⟨https://www.weforum.org/agenda/2020/07/tackling-the-hard-to-abate-sectors-join-the-conversation/⟩, (Accessed 17 May 2022).
[4] Negative Emissions Technologies and Reliable Sequestration: A Research Agenda | The National Academies Press. ⟨https://nap.nationalacademies.org/catalog/25259/negative-emissions-technologies-and-reliable-sequestration-a-research-agenda⟩, (Accessed 17 May 2022).
[5] N. McQueen, et al., Cost analysis of direct air capture and sequestration coupled to low-carbon thermal energy in the United States, Environ. Sci. Technol. 54 (12) (2020) 7542–7551, https://doi.org/10.1021/acs.est.0c00476.
[6] Carbon Engineering, Direct Air Capture of CO2, Home. ⟨https://carbonengineering.com/⟩, (Accessed 17 May 2022).
[7] Achieve Net Zero Targets with Climeworks Direct Air Capture. ⟨https://climeworks.com/⟩, (Accessed 17 May 2022).
[8] Global Thermostat. ⟨https://globalthermostat.com/⟩, (Accessed 17 May 2022).
[9] S. Deutz, A. Bardow, Life-cycle assessment of an industrial direct air capture process based on temperature–vacuum swing adsorption, no. 2, Art, Nat. Energy 6 (2) (2021), https://doi.org/10.1038/s41560-020-00771-9.
[10] T. Terlouw, K. Treyer, C. Bauer, M. Mazzotti, Life cycle assessment of direct air carbon capture and storage with low-carbon energy sources, Environ. Sci. Technol. 55 (16) (2021) 11397–11411, https://doi.org/10.1021/acs.est.1c03263.
[11] D.W. Keith, G. Holmes, D.S. Angelo, K. Heidel, A process for capturing CO_2 from the atmosphere, Joule 2 (8) (2018) 1573–1594, https://doi.org/10.1016/j.joule.2018.05.006.
[12] J.M. Greene, D. Quiroz, S. Compton, P.J. Lammers, J.C. Quinn, A validated thermal and biological model for predicting algal productivity in large scale outdoor cultivation systems, Algal Res 54 (2021) 102224, https://doi.org/10.1016/j.algal.2021.102224.
[13] P.H. Chen, J.C. Quinn, Microalgae to biofuels through hydrothermal liquefaction: open-source techno-economic analysis and life cycle assessment, Appl. Energy 289 (2021), 116613, https://doi.org/10.1016/j.apenergy.2021.116613.
[14] B.M. McInnis, J.D. Hurt, S. McDaniel, L.K. Kemp, T.W. Hodges, D.R. Nobles Jr., Carbon Capture Coatings: Proof of Concept Results and Call to Action, Coatings World, 2019. ⟨https://www.coatingsworld.com/issues/2019-07-01/view_technical-papers/carbon-capture-coatings-proof-of-concept-results-and-call-to-action/⟩, (Accessed 13 September 2022).
[15] D.R. Nobles, R.M. Brown, Transgenic expression of Gluconacetobacter xylinus strain ATCC 53582 cellulose synthase genes in the cyanobacterium Synechococcus leopoliensis strain UTCC 100, Cellulose 15 (5) (2008) 691–701, https://doi.org/10.1007/s10570-008-9217-5.
[16] D.C. Ducat, J.A. Avelar-Rivas, J.C. Way, P.A. Silver, Rerouting carbon flux to enhance photosynthetic productivity, Appl. Environ. Microbiol. 78 (8) (2012) 2660–2668, https://doi.org/10.1128/AEM.07901-11.
[17] O.I. Bernal, C.B. Mooney, M.C. Flickinger, Specific photosynthetic rate enhancement by cyanobacteria coated onto paper enables engineering of highly reactive cellular biocomposite 'leaves': highly reactive cyanobacteria biocomposites, Biotechnol. Bioeng. 111 (10) (2014) 1993–2008, https://doi.org/10.1002/bit.25280.
[18] L.K. Kemp, T.W. Hodges, L.B. Howard, S. McDaniel, Carbon capture coatings, in: Proceedings of the Annual International Waterborne, High-Solids, and Powder Coatings Symposium, Hattiesburg, Mississippi, 2020, pp. 235–247.
[19] S. McDaniel, B.M. McLnnis, T.W. Hodges, L.K. Kemp, Ammonia-generating coatings: truly green, Eur. Coat. J., 2020. [Online]. Available: ⟨https://360.european-coatings.com/journals/ammonia-generating_coatings_truly_green–EC_626181fe577bdc0027a864f9bf5a3b7756c31a62⟩.
[20] M. Kobašlija, D.T. McQuade, Removable colored coatings based on calcium alginate hydrogels, Biomacromolecules 7 (8) (2006) 2357–2361, https://doi.org/10.1021/bm060341q.
[21] M. Cibinel, G. Pugliese, D. Porrelli, L. Marsich, V. Lughi, Recycling alginate composites for thermal insulation, Carbohydr. Polym. 251 (2021), 116995, https://doi.org/10.1016/j.carbpol.2020.116995.
[22] R.E. Sousa, C.M. Costa, S. Lanceros-Méndez, Advances and future challenges in printed batteries, ChemSusChem 8 (21) (2015) 3539–3555, https://doi.org/10.1002/cssc.201500657.
[23] K.P. Musselman, C.F. Uzoma, M.S. Miller, Nanomanufacturing: high-throughput, cost-effective deposition of atomic scale thin films via atmospheric pressure spatial atomic layer deposition, Chem. Mater. 28 (23) (2016) 8443–8452, https://doi.org/10.1021/acs.chemmater.6b03077.
[24] The AMSA 2002 Financial Survey, p. 326.
[25] A. Dutta et al., Process Design and Economics for the Conversion of Lignocellulosic Biomass to Hydrocarbon Fuels. Thermochemical Research Pathways with In Situ and Ex Situ Upgrading of Fast Pyrolysis Vapors, National Renewable Energy Lab. (NREL), Golden, CO (United States), NREL/TP-5100-62455, 2015. doi: ⟨10.2172/1215007⟩.
[26] R. Davis, J. Markham, C. Kinchin, N. Grundl, E.C.D. Tan, D. Humbird, Process Design and Economics for the Production of Algal Biomass: Algal Biomass Production in Open Pond Systems and Processing Through Dewatering for Downstream Conversion, NREL/TP–5100-64772, 1239893, 2016. doi: ⟨10.2172/1239893⟩.
[27] F. Fasaei, J.H. Bitter, P.M. Slegers, A.J.B. van Boxtel, Techno-economic evaluation of microalgae harvesting and dewatering systems, Algal Res. 31 (2018) 347–362, https://doi.org/10.1016/j.algal.2017.11.038.
[28] A. Akhtar, I. Jiříček, T. Ivanova, A. Mehrabadi, V. Krepl, Carbon conversion and stabilisation of date palm and high rate algal pond (microalgae) biomass through slow pyrolysis, Int. J. Energy Res 43 (9) (2019) 4403–4416, https://doi.org/10.1002/er.4565.
[29] M. Ahmad, et al., Date palm waste-derived biochar composites with silica and zeolite: synthesis, characterization and implication for carbon stability and recalcitrant potential, Environ. Geochem. Health 41 (4) (2019) 1687–1704, https://doi.org/10.1007/s10653-017-9947-0.
[30] V. Pidlisnyuk, R.A. Newton, A. Mamirova, Miscanthus biochar value chain - a review, J. Environ. Manag. 290 (2021), 112611, https://doi.org/10.1016/j.jenvman.2021.112611.
[31] P.H. Brunner, P.V. Roberts, The significance of heating rate on char yield and char properties in the pyrolysis of cellulose, Carbon 18 (3) (1980) 217–224, https://doi.org/10.1016/0008-6223(80)90064-0.
[32] C. Zhang, et al., Pyrolysis of cellulose: evolution of functionalities and structure of bio-char versus temperature, Renew. Sustain. Energy Rev. 135 (C) (2021). Accessed: Oct. 27, 2022. [Online]. Available: https://ideas.repec.org/a/eee/rensus/v135y2021ics1364032120307036.html.
[33] K.A. Spokas, Review of the stability of biochar in soils: predictability of O:C molar ratios, Carbon Manag. 1 (2) (2010) 289–303, https://doi.org/10.4155/cmt.10.32.
[34] K.M. Weyer, D.R. Bush, A. Darzins, B.D. Willson, Theoretical maximum algal oil production, BioEnergy Res. 3 (2) (2010) 204–213, https://doi.org/10.1007/s12155-009-9046-x.
[35] Solar Resource Maps of World. ⟨https://solargis.com/maps-and-gis-data/download/world⟩, (Accessed 19 May 2022).
[36] The Chemical Engineering Plant Cost Index – Chemical Engineering. ⟨https://www.chemengonline.com/pci-home⟩, (Accessed 31 January 2020).
[37] Comparing the Profitability of a Greenhouse to a Vertical Farm in Quebec – Eaves – 2018, Can. J. Agric.l Econ./Revue canadienne d'agroeconomie – Wiley Online Library. ⟨https://onlinelibrary.wiley.com/doi/full/10.1111/cjag.12161?casa_token=iKGldhBU4owAAAAA%3A4eMKDGZiBy6lAIyMEl71zX0QmzTMT9Yd2JYYd9

671YAX0DcEQavYznVIU74HARsGl9GoLHg0bixt-iM⟩, (Accessed 6 September 2022).
[38] High Speed 8 Colors Offset Rotogravure Printing Machine 7 Motor Control Printing Unit For Food Package, Plastic Film – Buy 8 Colors Rotogravure Printing Machine, High Speed Rotogravure Printing Machine 7 Motor Control, Rotogravure Printing Machine Press Unit For Plastic Film Product on Alibaba.com. ⟨https://www.alibaba.com/product-detail/Rotogravure-Printing-Machine-Film-Printing-Machine_1600329192283.html?spm=a2700.7724857.0.0.5efe451ctWSR4A&s=p⟩, (Accessed 6 September 2022).
[39] Forklift Pricing 101: What You Should Know, Toyota Forklifts. ⟨https://www.toyotaforklift.com/resource-library/material-handling-solutions/finance/forklift-pricing-101-what-you-should-know⟩, (Accessed 6 September 2022).
[40] How Much Does a Semi-Truck Cost?, Rechtien International Trucks. ⟨https://www.rechtien.com/how-much-does-a-semi-truck-cost/⟩, (Accessed 6 September 2022).
[41] SunShot 2030, Energy.gov. ⟨https://www.energy.gov/eere/solar/sunshot-2030⟩, (Accessed 8 August 2022).
[42] Gasoline and Diesel Fuel Update. ⟨https://www.eia.gov/petroleum/gasdiesel/index.php⟩, (Accessed 8 August 2022).
[43] 2019 Cost of Clean Water Index, The National Association of Clean Water Agencies.
[44] China Factory Direct Supply Construction Building Safety Pe Net Mesh – Buy Construction Safety Mesh,Safety Pe Mesh,Building Safety Mesh Product on Alibaba.com. ⟨https://www.alibaba.com/product-detail/Mesh-China-Factory-Direct-Supply-Construction_1600601639956.html?spm=a2700.galleryofferlist.normal_offer.d_title.69b237ebFg5seC&s=p⟩, (Accessed 6 September 2022).
[45] Y. Zhu, S.B. Jones, D.B. Anderson, Algae Farm Cost Model: Considerations for Photobioreactors, Pacific Northwest National Lab. (PNNL), Richland, WA (United States), PNNL-28201, Oct. 2018. doi: ⟨10.2172/1485133⟩.
[46] Bulk Food Additives Ingredients Ensign Trisodium Sodium Citrate Tsc Sodium Citrate – Buy Rzbc/ensign/weifang/ttca Citric Acid Anhydrous/citric Acid Monohydrate/trisodium Citrate/sodium Citrate,Sodium Citrate Formula Trisodium Citrate For Free Drinks,Bulk Food Additives Ingredients Ensign Trisodium Sodium Citrate Tsc Sodium Citrate Product on Alibaba.com. ⟨https://www.alibaba.com/product-detail/Bulk-Food-Additives-Ingredients-ENSIGN-Trisodium_1600609204658.html?spm=a2700.galleryofferlist.normal_offer.d_title.354050aeDWEVFZ⟩, (Accessed 6 September 2022).
[47] Ethylene Diamine Tetraacetic Acid Edta Detergent Grade – Buy Ethylene Diamine Tetraacetic Acid, Edta, Edta 2na Product on Alibaba.com. ⟨https://www.alibaba.com/product-detail/Ethylene-Diamine-Tetraacetic-Acid-EDTA-Detergent_1600393298045.html?spm=a2700.7724857.0.0.37e57c68xI39LF⟩, (Accessed 6 September 2022).
[48] The Price Of Liquid Nitrogen In The United States, Rutherford & Titan. ⟨https://www.rutherfordtitan.com/liquid-nitrogen-generators/liquid-nitrogen-price-usa/⟩, (Accessed 6 September 2022).
[49] The Economic Value of Biochar in Crop Production and Carbon Sequestration – ScienceDirect. ⟨https://www.sciencedirect.com/science/article/abs/pii/S0301421511005672?via%3Dihub⟩, (Accessed 6 September 2022).
[50] ILO Data Explorer. ⟨https://www.ilo.org/shinyapps/bulkexplorer15/?lang=en&segment=indicator&id=EAR_4MTH_SEX_ECO_CUR_NB_A⟩, (Accessed 6 September 2022).
[51] K.-M. Lee, A. Inaba, Life Cycle Assessment Best Practices of ISO 14040 Series, 2004, [Online]. Available: ⟨https://www.apec.org/-/media/APEC/Publications/2004/2/Life-Cycle-Assessment-Best-Practices-of-International-Organization-for-Standardization-ISO-14040-Ser/04_cti_scsc_lca_rev.pdf⟩.
[52] G. Wernet, C. Bauer, B. Steubing, J. Reinhard, E. Moreno-Ruiz, B. Weidema, The ecoinvent database version 3 (part I): overview and methodology, Int. J. Life Cycle Assess. 21 (9) (2016) 1218–1230, https://doi.org/10.1007/s11367-016-1087-8.
[53] World Bank, State and Trends of Carbon Pricing 2021. The World Bank, 2021. doi: ⟨10.1596/978-1-4648-1728-1⟩.